Journal of Optometry 19 (2026) 100632

Contents lists available at ScienceDirect

Journal of Optometry

journal homepage: www.journalofoptometry.org

Original Article

Analysis of the factors influencing the treatment zone area after overnight orthokeratology lens wearing

Xinda Li [a,b,c,d], Yue Xin [a,c,d], Zonghan Zhou [a,c,d], Jingjing Zong [a,b,c,d], Lijun Zhang [a,c,d,*]

[a] The Third People's Hospital of Dalian University of Technology, Dalian, China
[b] Dalian Medical University, Dalian, China
[c] Liaoning Key Laboratory of Cornea and Ocular Surface, Dalian, China
[d] Liaoning Provincial Optometry Technology Engineering Research Center, Dalian, China

ARTICLE INFO

Keywords:
Orthokeratology
Treatment zone
Myopia
Factor
Vision shaping treatment
Corneal refractive therapy

ABSTRACT

Purpose: To identify the influencing factors of the treatment zone area (TZA) after overnight orthokeratology (OK) lens wearing, and validate an integrated open source workflow using R language (R) for measuring treatment zone parameters.

Methods: The retrospective study included 239 children (7–16 years) who wore OK lenses continuously for 12 months. Two OK lens designs were used: 1) Vision Shaping Treatment (VST) lenses, with back optic (BC) zone diameters of 5.5 mm or 6.0 mm; 2) Corneal Refractive Therapy (CRT) lenses, with BC zone diameters of 5.0 mm or 6.0 mm. Patients were divided into four groups based on lens design and BC zone diameter: VST-S (5.5 mm, $n = 61$), VST-L (6.0 mm, $n = 66$), CRT-S (5.0 mm, $n = 59$), and CRT-L (6.0 mm, $n = 53$). Treatment zone parameters were quantified using R and MATLAB. Spearman correlation analysis and multiple linear regression were applied to explore factors influencing TZA.

Results: R and MATLAB showed high agreement in measuring treatment zone parameters: Cronbach's alpha values were 0.993 for treatment zone decentration (TZD) and 0.991 for TZA; intraclass correlation coefficient values were 0.986 for TZD and 0.983 for TZA. TZA, semimajor axis (a), semiminor axis (b), ellipse eccentricity (e), and tilt angle of the fitted ellipses (alpha) were significantly correlated with TZD ($P < 0.05$). Post hoc comparisons revealed VST-L group had significantly larger TZA than the other three groups (all $P < 0.001$); TZA of VST-L group was significantly larger than that of CRT-L group ($U = 719.000$, $P < 0.001$). Corneal mean keratometry change (Δkm), TZD, shape factor change (Δp), preoperative p, and BC zone diameter were independent predictors of TZA ($R^2 = 0.730$), with Δkm showing the strongest correlation (Standardized Coefficients = 0.963).

Conclusion: R is reliable for measurement of treatment zone parameters, with results consistent with MATLAB. The vector of decentration aligned closer with the direction of semiminor axis of the fitted treatment zone ellipse, and greater ellipse eccentricity was associated with greater treatment zone decentration. Δkm, TZD, Δp, preoperative p, and BC zone diameter were independently associated with TZA. These findings characterize factors associated with treatment zone morphology and may inform future prospective studies of individualized orthokeratology lens fitting.

Introduction

Myopia has become one of the most significant challenges in global public health. One cross-sectional study suggested that the myopia rate among Chinese primary school children could be as high as 68.78%. Furthermore, it is projected that by 2050, up to 49.8% of the global population could have myopia, with high myopia affecting 9.8% of the population.[1,2] Early engagement in near-work activities and insufficient outdoor time are major risk factors for the development of myopia.[3] High myopia is associated with several irreversible blinding eye diseases.[4] Consequently, preventing myopia and slowing its progression in children and adolescents is a major research focus.

Orthokeratology (OK) lenses have been proven to be safe, effective, and reversible interventions for myopia.[5–7] These are corneal contact lenses featuring a reverse-geometry design. Overnight wear reshapes the cornea to create a multifocal surface, flattening the central curvature and steepening the mid-peripheral curvature. The treatment zone is the relatively flattened central area of the anterior corneal surface. It provides the best visual quality and minimal aberrations as light passes through. Previous studies have indicated that its area (Treatment Zone

*Corresponding author at: The Third People's Hospital of Dalian University of Technology, Dalian, China.
E-mail address: Lijunzhangw1970@163.com (L. Zhang).

https://doi.org/10.1016/j.optom.2026.100632
Received 8 April 2026; Accepted 20 July 2026

1888-4296/© 2026 Published by Elsevier España, S.L.U. on behalf of Spanish General Council of Optometry. This is an open access article under the CC BY-NC-ND license (http://creativecommons.org/licenses/by-nc-nd/4.0/)

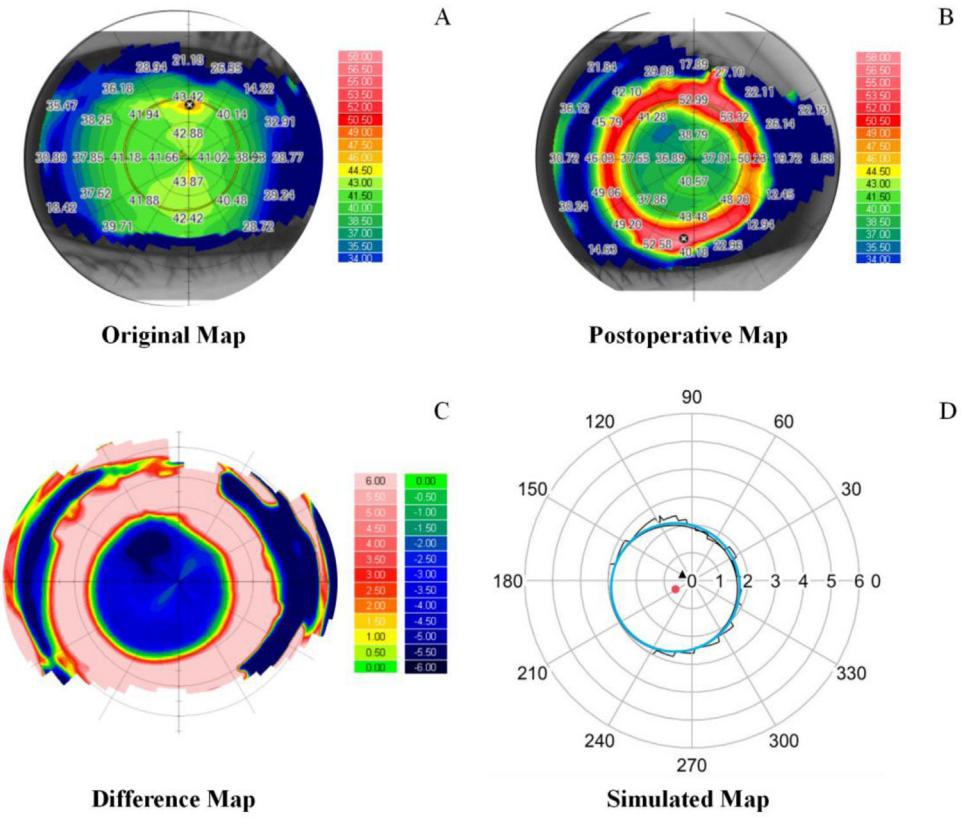

Fig. 1. Strategy to determine the TZD and TZA. A. Baseline original tangential curvature map; B. Postoperative tangential curvature map at the twelve-month visit; C. Difference tangential curvature map; D. Simulated difference map by R; the black triangle represents the pupil center, the blue ring indicates the fitted treatment zone, and the red circle indicates the center of the fitted treatment zone. The distance between the black triangle and red circle is defined as the TZD. The area of the blue ring is defined as the TZA. TZA: treatment zone area; TZD: treatment zone decentration; R: software for statistics and plotting, version 4.2.2, http://www.R-project.org/.

Area, TZA) is closely related to myopia control efficacy.[8–10] Clinically, reducing the back optic (BC) zone diameter of OK lenses is a common strategy to shrink the TZA. However, in practice, the TZA alone cannot be precisely controlled. This suggests that other factors influence the TZA, which are not yet fully understood.

Currently, most studies rely on engineering software such as MATLAB for TZA quantification.[11,12] While MATLAB is highly robust for matrix computations and topographic data extraction, transitioning from image processing in MATLAB to subsequent clinical statistical analysis often requires researchers to switch between different software environments. R language (R) is an open-source platform that has seen widespread adoption in biomedical and health sciences research.[13] Although other open-source alternatives, such as Python, offer comparable programming capabilities, R was specifically selected for this study due to its extensive ecosystem of specialized biostatistical packages and its higher familiarity among clinical researchers and biostatisticians.[13,14] Establishing a unified workflow in R that encompasses both topography data processing and downstream clinical modeling would substantially streamline the research process. However, the feasibility of using R to process raw corneal topography data and calculate the TZA has not yet been validated against established platforms like MATLAB.

Additionally, the mechanism by which OK lenses alter corneal shape remains unclear. The prevailing view is that corneal epithelial remodeling is the core process involved.[15–17] Quantifying this epithelial remodeling at the cellular level is challenging. On the basis of the current literature, most studies calculate central epithelial thinning or mid-peripheral thickening to reflect the extent of remodeling. However, parameters quantifying the intrinsic relationship between these changes are rarely reported.[18–20]

Therefore, this study developed a TZA quantification method using R. This method aims to validate its agreement with traditional MATLAB analysis. This study also investigated the size and influencing factors of the TZA generated by different OK lens designs and different BC zones after one year of wear.

Method

Subjects

This was a retrospective study. Patients fitted with OK lenses at The Third People's Hospital of Dalian University of Technology between October 2020 and October 2024 were enrolled. The inclusion criteria were as follows: 1) continuous OK lens wear for more than 12 months;

Table 1
Agreement assessment between R and MATLAB.

Parameter	Cronbach's alpha	ICC	95% Confidence Interval Lower	95% Confidence Interval Upper	*P* value
TZD	0.993	0.986	0.982	0.989	<0.001
TZA	0.991	0.983	0.978	0.986	<0.001

TZD: treatment zone decentration; TZA: treatment zone area; ICC: intraclass correlation coefficient.

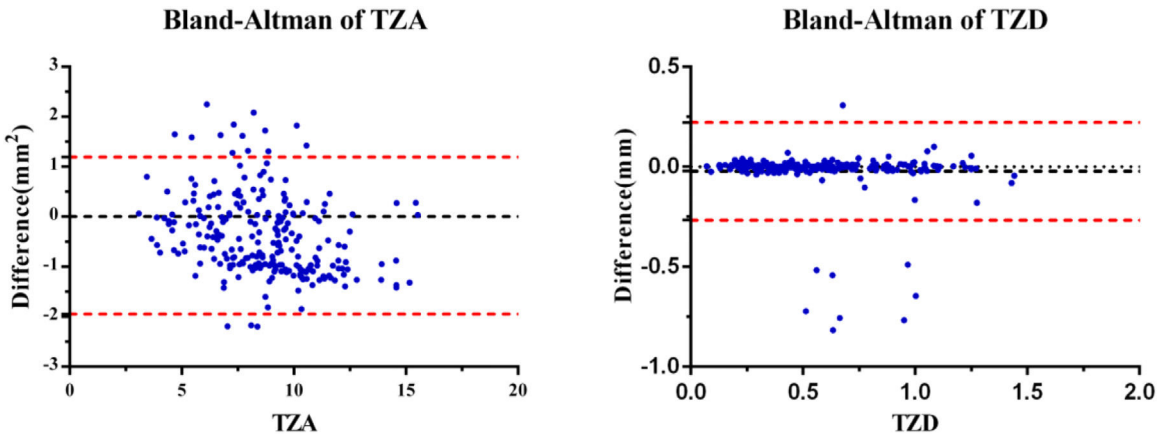

Fig. 2. Bland–Altman plot of TZA and TZD. TZA: treatment zone area; TZD: treatment zone decentration.

2) age 7−16 years; 3) cycloplegic refraction: −6.00 D ≤ spherical power ≤ 0.00 D, cylindrical power ≤ 1.50 D; 4) flat keratometry (K) value between 39.00 D and 46.00 D; and 5) best-corrected visual acuity ≥ 20/20. The exclusion criteria were as follows: 1) strabismus, amblyopia, other systemic or ocular diseases, or trauma unsuitable for lens wear; 2) history of ocular surgery or other contact lens wear; and 3) concurrent use of low-dose atropine. The study was approved by the Ethics Committee of The Third People's Hospital of Dalian University of Technology (Approval No. 2024-170-002).

Orthokeratology lens fitting and parameter examination

Two OK lens designs were used: 1) Corneal refractive therapy (CRT) lenses use a three-zone design: a base curve zone adjusting the central curvature, a reverse zone for lens centration, and a landing zone aligning the lens edge. CRT lenses (Paragon Vision Sciences) have an oxygen permeability (Dk) of $100*10^{-11}$ (cm^2/s) ($mLO_2/mL{\cdot}mmHg$). The total lens diameter ranged from 10.0 mm to 11.5 mm, with optical zones of 5.0 mm or 6.0 mm. 2) Vision shaping treatment (VST) lenses use a four-zone design: a central base curve, a paracentral reverse curve, a peripheral alignment curve, and a peripheral landing zone. Two brands of VST design lenses were used: myOK (Brightenoptix), with a Dk of $141*10^{-11}$ (cm^2/s) ($mLO_2/mL{\cdot}mmHg$), and SDJ (SDJMASTERVISION), with a Dk of $127*10^{-11}$ (cm^2/s) ($mLO_2/mL{\cdot}mmHg$). The total diameter also ranged from 10.0 mm to 11.5 mm, with optical zones of 5.5 mm or 6.0 mm. Lens fitting strictly followed the manufacturers' guidelines. A slit-lamp biomicroscope and corneal topography were used to assess the fitting effect. Lens parameters were adjusted to achieve a typical bull's eye fluorescein pattern and ensure approximately 1 mm of lens movement. Patients were instructed to wear the lenses overnight for at least 8 h, for a minimum of 6 nights per week. All patients were scheduled for follow-up visits before lens wear and at 1 day, 1 week, 1 month, 3 months, 6 months, and 12 months after wearing the lenses. Baseline examinations included uncorrected visual acuity (UCVA), best-corrected visual acuity (BCVA), cycloplegic autorefraction, noncontact tonometry, corneal topography, slit-lamp anterior segment examination, pupil radius measurement, axial length measurement, ocular alignment, and dominant eye assessment. Cycloplegic autorefraction was measured via an autorefractor (AR-1, Nidek). This was performed 30 min after instilling one drop of compound tropicamide eye drops every 5 min, for a

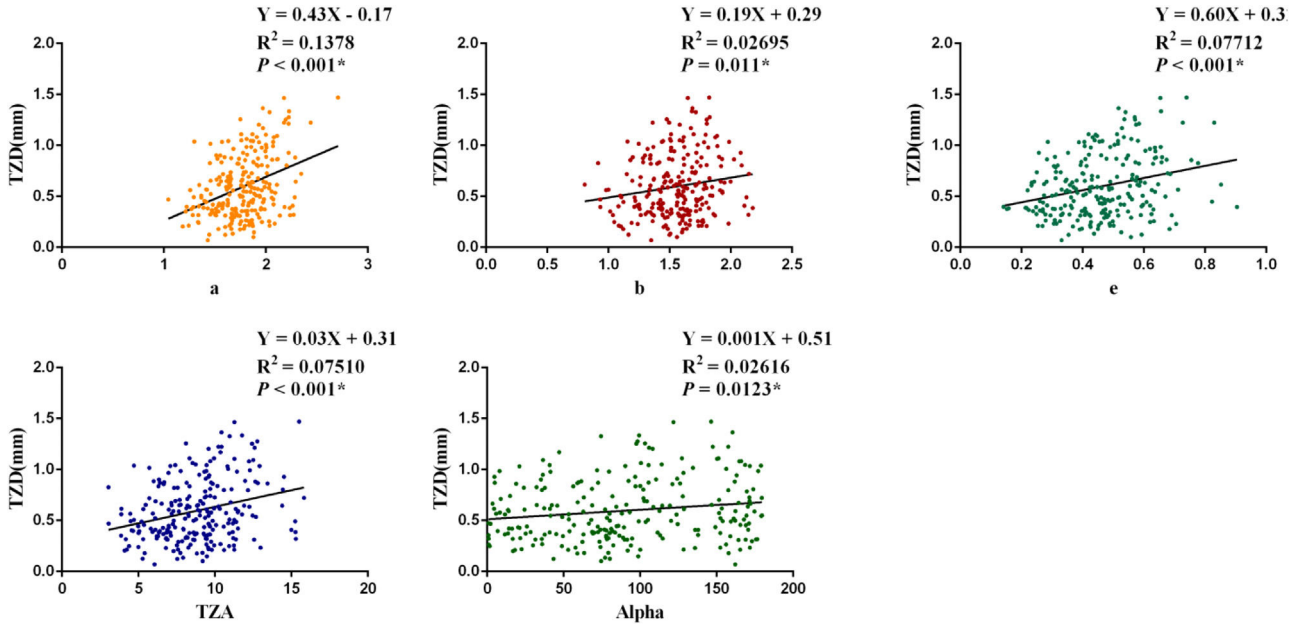

Fig. 3. Factors Related to Treatment Zone Decentration (TZD). a: semimajor axis; b: semiminor axis; e: ellipse eccentricity; TZA: treatment zone area; Alpha: tilt angle of the fitted ellipses; * indicates statistical significance.

Table 2
Baseline characteristics.

Parameter	VST-S $n = 61$	VST-L $n = 66$	CRT-S $n = 59$	CRT-L $n = 53$	*P* value
Age(y)	9.98 ± 1.82	10.55 ± 2.08	9.85 ± 1.95	10.45 ± 2.23	0.142
Sex(F/M)	35/26	33/33	29/30	26/27	0.763
SE(D)	−2.25 ± 1.16	−2.60 ± 1.46	−2.72 ± 1.59	−2.37 ± 1.45	0.420
p	0.76 ± 0.13	0.76 ± 0.09	0.73 ± 0.08	0.73 ± 0.08	0.006[a]
km(mm)	7.81 ± 0.25	7.80 ± 0.23	7.80 ± 0.22	7.86 ± 0.22	0.466
ApexCT(μm)	590.61 ± 51.35	592.16 ± 59.62	600.23 ± 67.67	606.57 ± 67.10	0.649
CCT(μm)	559.98 ± 28.26	560.29 ± 31.75	569.84 ± 37.92	572.27 ± 33.94	0.090

VST-S: VST small group; VST-L: VST large group; CRT-S: CRT small group; CRT-L: CRT large group; SE: spherical equivalent; p: shape factor; km: mean keratometry; ApexCT: corneal thickness at the corneal apex; CCT: central corneal thickness.
[a] No significant difference after Bonferroni correction.

Table 3
Factors related to treatment zone decentration.

	Spearman's correlation		Multiple Linear Regression
	ρ	*P* value	*P* value
TZA	0.250	<0.001	
a	0.309	<0.001	<0.001
b	0.153	0.018	
e	0.245	<0.001	<0.001
alpha	0.153	0.018	0.018

TZA: treatment zone area; a: semimajor axis; b: semiminor axis; e: ellipse eccentricity; alpha: the tilt angle of the fitted ellipses.

total of three drops. The spherical equivalent (SE) was calculated as sphere + 1/2 cylinder. Corneal parameters were measured via a Sirius corneal topographer (CSO, Italy) under consistent mesopic lighting (40 lx). The measured parameters included mean keratometry (km, expressed in millimeters), corneal thickness at the corneal apex (ApexCT), central corneal thickness, and shape factor (p), which serves as a geometric metric to quantify corneal asphericity. All measurements were taken by an experienced technician from the same team. Δkm was defined as the postoperative km minus the preoperative km. Δp represents the postoperative p minus the preoperative p. ΔApexCT represents the postoperative ApexCT value minus the preoperative ApexCT value. ΔCCT (central corneal thickness) was the postoperative CCT minus the preoperative CCT.

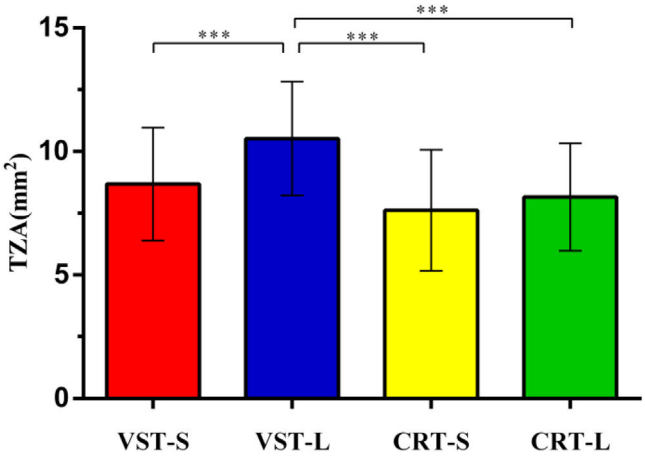

Fig. 4. Treatment Zone Area (TZA) among the four groups. VST-S: VST small group; VST-L: VST large group; CRT-S: CRT small group; CRT-L: CRT large group.*** indicates statistical significance.

Treatment zone parameters

The treatment zone was defined as the central corneal area with optimal optical quality following orthokeratology lens wear, specifically delineated as a continuous region where the tangential curvature decreases by ≥0.00 D compared to the pre-operative baseline. Its boundary was determined by the isoline where the curvature difference equals 0.00 D. Parameter quantification followed a strictly standardized data processing protocol: this study exported baseline data (Fig. 1A) and raw tangential corneal curvature data after 12 months of lens wear (Fig. 1B)

Table 4
Postwear outcomes.

Parameter	VST-S $n = 61$	VST-L $n = 66$	CRT-S $n = 59$	CRT-L $n = 53$	*P* value
TZA(mm^2)	8.68 ± 2.29	10.52 ± 2.31	7.62 ± 2.45	8.16 ± 2.17	<0.001
km(mm)	8.01 ± 0.28	8.08 ± 0.28	8.04 ± 0.29	8.12 ± 0.31	0.187
ApexCT(μm)	612.38 ± 45.22	626.17 ± 37.56	641.63 ± 51.80	654.03 ± 46.60	<0.001
CCT(μm)	553.30 ± 28.82	552.21 ± 31.32	564.98 ± 39.27	566.47 ± 34.28	0.032[a]
p	1.75 ± 0.60	1.98 ± 0.57	2.21 ± 0.52	2.04 ± 0.56	<0.001
Δkm(mm)	0.20 ± 0.19	0.27 ± 0.21	0.24 ± 0.22	0.26 ± 0.17	0.172
ΔApexCT(μm)	21.76 ± 49.73	34.01 ± 54.05	41.40 ± 44.98	47.46 ± 53.03	0.003
ΔCCT(μm)	−6.68 ± 9.28	−8.09 ± 12.06	−4.86 ± 11.69	−5.80 ± 17.12	0.371
Δp	0.99 ± 0.59	1.22 ± 0.58	1.49 ± 0.52	1.32 ± 0.57	<0.001

VST-S: VST small group; VST-L: VST large group; CRT-S: CRT small group; CRT-L: CRT large group; TZA: treatment zone area; km: mean keratometry; ApexCT: corneal thickness at the corneal apex; CCT: central corneal thickness; p: shape factor; Δ: difference between post-operative and pre-operative (post minus pre).
[a] No significant difference after Bonferroni correction.

Table 5
Factors related to treatment zone area.

	ρ	*P* value
Lens Design	−0.359	<0.001
BC zone diameter	0.288	<0.001
TZD	0.250	<0.001
preoperative p	0.184	0.004
Δkm	0.623	<0.001
ΔCCT	−0.195	0.002
Δp	0.159	0.014

BC: back optic; TZD: treatment zone decentration; p: shape factor; km: mean keratometry; CCT: central corneal thickness; Δ: difference between post-operative and pre-operative (post minus pre).

in .csv format from the Sirius corneal topographer. Each data file covered a circular area with a 6 mm radius, comprising 256 × 31 measurement points with an adjacent point spacing of 0.2 mm. The point-by-point tangential curvature data from both the baseline and post-operative periods were imported into a custom analysis script written in R (version 4.2.2, https://www.R-project.org) and MATLAB. The curvature difference for each point was calculated point-by-point, as illustrated in Fig. 1C. For all data points extending from the corneal apex to the periphery, the curvature difference theoretically transitions from a negative value to a positive value, and then back to a negative value. Therefore, the boundary point of the treatment zone in any given meridian was defined as the first point where the curvature difference equaled 0.00 D. This process was repeated for data across all meridians. The discrete boundary points with ΔK = 0.00 D identified across all directions were then fitted to a standard geometric elliptical model using the least squares method (Fig. 1D). To robustly handle off center treatment zones, the center coordinates of the ellipse were treated as independent free parameters during the optimization process, ensuring that the R workflow maintains the same alignment precision as MATLAB when the topography geometry is not concentric. Based on these fitting results, the geometric center of the fitted ellipse was defined as the Treatment Zone Center (TZC). Treatment Zone Decentration (TZD) was defined as the distance between the TZC and the pupillary center. The Treatment Zone Area (TZA) was calculated as the total geometric area encompassed within the fitted ellipse.

Statistical analysis

To avoid strong correlations between eyes, only data from the right eye were used for subsequent statistical analysis in bilateral lens wearers. The Shapiro–Wilk test was used for normality testing, and Levene's test was used for homogeneity of variance. Normally distributed data were compared via t tests or ANOVA; nonnormally distributed data were compared between two groups via the Mann–Whitney U test and among multiple groups via the Kruskal–Wallis test; categorical data were analyzed via the chi–square test. Post hoc comparisons were

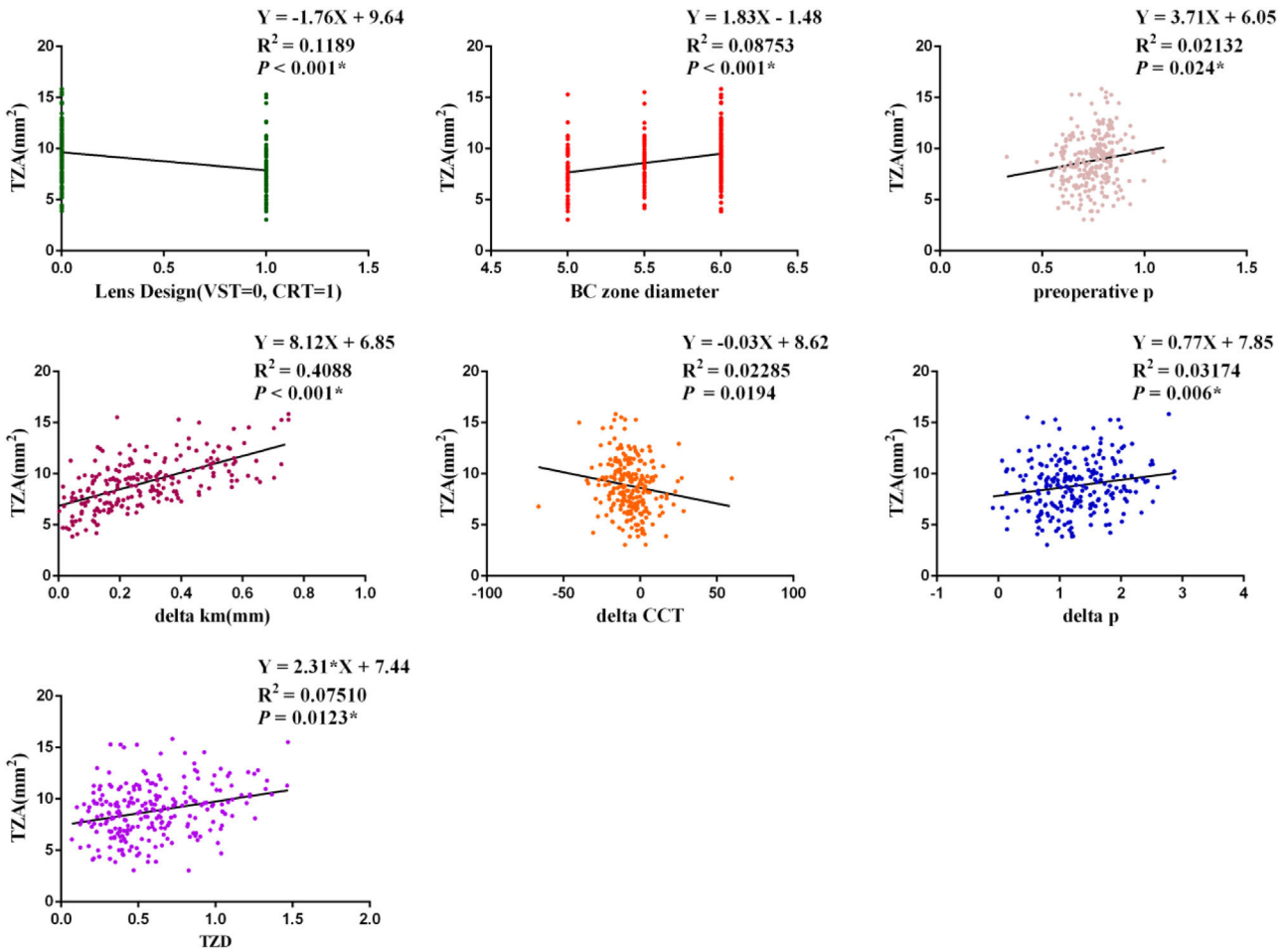

Fig. 5. Factors Related to Treatment Zone Area (TZA). BC: back optic; p: shape factor; km: mean keratometry; CCT: central corneal thickness; delta: difference between post-operative and pre-operative (post minus pre); TZD: treatment zone decentration; * indicates statistical significance.

Table 6
Multiple linear regression analysis for treatment zone area.

Parameter	B	Standard Error	Standardized Coefficients	t	*P* value	VIF
Δkm	12.243	0.597	0.963	20.500	<0.001	1.950
TZD	3.686	0.323	0.437	11.413	<0.001	1.296
Δp	−1.142	0.211	−0.263	−5.408	<0.001	2.091
preoperative p	2.822	0.870	0.111	3.242	0.001	1.037
BC zone diameter	0.647	0.217	0.105	2.978	0.003	1.090

Model fit: $R^2 = 0.730$ km: mean keratometry; TZD: treatment zone decentration; p:shape factor; BC: back optic; Δ: difference between post-operative and pre-operative (post minus pre).

performed via the Bonferroni correction. Spearman's correlation coefficient and multiple linear regression were used to analyze the factors influencing the TZA. The intraclass correlation coefficient (ICC) and Cronbach's alpha were used to evaluate the agreement between the two measurement methods for the treatment zone parameters. All the data were presented as the means ± standard deviations. To ensure OK lens stabilization, the TZD and TZA calculations used data from the 12-month visit.[21,22] Statistical analysis was performed via SPSS (version 26.0.0.0; IBM, ibm.com). A P value < 0.05 was considered statistically significant.

Results

Baseline

This study included 239 patients (239 eyes). Among them, 123 were female and 116 were male. The mean age was 10.18 ± 2.04 years; the mean SE was −2.49 ± 1.43 D; the mean p value was 0.75 ± 0.10; the mean km was 7.82 ± 0.23 mm; the mean ApexCT was 596.95 ± 61.44 μm; the mean CCT was 565.23 ± 33.30 μm. Patients were divided into the VST-S group (5.5 mm, n = 61), VST-L group (6.0 mm, n = 66), CRT-S group (5.0 mm, n = 59), and CRT-L group (6.0 mm, n = 53) on the basis of the OK lens design and BC zone diameter.

Agreement assessment

The TZD measured by R was 0.60 ± 0.30 mm, and the TZA was 8.81 ± 2.56 mm^2. The TZD measured by MATLAB was 0.60 ± 0.31 mm, and the TZA was 8.76 ± 2.40 mm^2. High agreement was observed between R and MATLAB for both the TZD and TZA measurements, with Cronbach's alpha values of 0.993 (TZD) and 0.991 (TZA) and ICC values of 0.986 (TZD) and 0.983 (TZA), as shown in Table 1. Bland–Altman plots revealed that for TZD, 96.23% of the points (230/239) were within the 95% limits of agreement. For the TZA, 94.56% of the points (226/239) were within the 95% limits of agreement (Fig. 2).

Given that the R framework demonstrated reliability in quantifying treatment zone metrics, all subsequent morphological analyses of the fitted ellipses were conducted exclusively using the integrated R workflow.

Characteristics of the treatment zone and relationship between TZD and treatment zone parameters

The mean semimajor axis (a) was 1.78 ± 0.26mm; the mean semiminor axis (b) was 1.55 ± 0.26mm; the mean ellipse eccentricity (e) was 0.46 ± 0.14; the mean tilt angle of the fitted ellipses (alpha) was 90.00 ± 53.00°.

TZD direction revealed that 129 cases 53.97 percent exhibited temporal-inferior decentration, and 58 cases 24.27 percent exhibited temporal-superior decentration. Additionally, 44 cases 18.41 percent showed nasal-inferior decentration, and 8 cases 3.35 percent showed nasal-superior decentration. To further elucidate the morphological characteristics of the treatment zone, an exploratory analysis was performed to evaluate the relationship between alpha and the distribution of decentration directions. Alpha was stratified into two categories: Group 1 (0° to 90°) and Group 2 (90° to 180°). The distribution of decentration quadrants was not identical between the two tilt angle groups (χ^2 = 10.187, $P < 0.05$). For temporal-inferior decentration, the rate in Group 2 was significantly higher than that in Group 1 (68.97% versus 31.03%, $P < 0.05$). Conversely, for temporal-superior decentration, Group 1 demonstrated a significantly higher rate than Group 2 (52.71% versus 47.29%, $P < 0.05$).

Spearman's correlation analysis revealed that TZA, a, b, e, and alpha were significantly correlated with TZD ($P < 0.05$), as shown in Table 3 and Fig. 3. Multiple linear regression analysis identified a, e, and alpha as independent influencing factors for TZD. All variance inflation factor (VIF) values were < 5.000.

Postwear outcomes

The baseline characteristics were not significantly different among the four groups (Table 2). The parameters at the 12-month visit were compared among the four groups in Table 4. The TZA was not identical across the four groups (H = 49.471, $P < 0.001$), as shown in Fig. 4. Post hoc comparisons revealed that the VST-L group differed significantly from the other three groups (all $P < 0.001$). No significant differences were found among the remaining groups. The TZA was significantly different between the VST design (127 eyes) and the CRT design (112 eyes) (U = 4155.000, $P < 0.001$). The TZA differed significantly between the VST-L and CRT-L groups (U = 719.000, $P < 0.001$).

Analysis of factors related to the TZA

Spearman's correlation analysis revealed that lens design, BC zone diameter, TZD, preoperative p, Δkm, ΔCCT, and Δp were significantly correlated with TZA size ($P < 0.05$), as shown in Table 5 and Fig. 5.

Multiple linear regression analysis identified Δkm, TZD, Δp, preoperative p, and BC zone diameter as independent influencing factors for TZA. All variance inflation factor (VIF) values were < 5.000. This model explained 73.0% of the variance in TZA size (R^2 = *0.730*), as shown in Table 6.

Discussion

Orthokeratology is a reversible, nonsurgical myopia correction method. It can suppress axial elongation by 30% to 63%.[23] Its efficacy and safety have been widely validated. OK lenses use their unique design to alter the corneal epithelial thickness profile. This reshapes the corneal curvature, creating a central treatment zone and a mid-peripheral defocus zone. This mechanism corrects myopia and slows its progression. Previous studies have demonstrated that a smaller TZA after OK lens wear enhances myopia control efficacy.[9,10,24] Therefore, establishing an accurate and convenient TZA quantification method is essential for a deeper investigation of its regulatory mechanism.

Previously, measuring treatment zone parameters often involved importing differential corneal topography data into MATLAB for fitting and calculation. MATLAB remains highly advantageous for complex matrix computations and robust image processing. However, a notable drawback in the clinical research context is the fragmented workflow;

researchers must often extract topographic data in MATLAB and then transition to separate statistical platforms for subsequent clinical modeling. Furthermore, recent bibliometric data demonstrate that R has achieved significantly wider adoption and familiarity than MATLAB within the health sciences and biomedical communities.[13,14] While Python presents another viable open-source alternative for image processing, R offers a distinct advantage for clinical researchers due to its extensive ecosystem of specialized biostatistical packages. Our study confirms that for both TZD and TZA, the Cronbach's alpha and ICC values between the R and MATLAB calculations were greater than 0.950. Thus, rather than replacing MATLAB due to unreliability, R provides an integrated, highly accessible, and accurate analytical alternative. It enables researchers to perform both precise boundary detection and downstream statistical analysis within a single unified platform.

The morphological evaluation of the treatment zone in this study revealed that the treatment zone exhibited prominent elliptical geometric characteristics rather than an ideal circular shape, with a mean e of 0.46. Regarding the spatial distribution of lens decentration, our data were highly consistent with classic clinical observations, demonstrating that displacement was predominantly clustered within the temporal-inferior quadrant 53.97% and the temporal-superior quadrant 24.27%. This phenomenon may be attributed to Bell phenomenon during sleep and the intrinsic asymmetry of the cornea.[25,26] Furthermore, chi square test results indicated that eyes with alpha between 0 and 90° primarily experienced temporal-superior decentration, whereas those with tilt angles between 90 and 180° were more susceptible to temporal-inferior decentration. Multiple linear regression analysis showed that the semi-major axis a, eccentricity e, and tilt angle alpha were independent factors influencing TZD. Notably, the vector of decentration aligned closer with the direction of the semiminor axis b of the ellipse, and a larger ellipse eccentricity e value was associated with a higher probability of decentration. Although the retrospective cross sectional nature of this study prevents the direct establishment of a causal relationship between elliptical morphology and decentration kinetics, we speculate that this localized mechanical compression may truncate the treatment zone boundary along the vector of lens displacement. The observed associations between ellipse morphology and TZD are directly supported by the present data, whereas their biomechanical interpretation remains hypothetical. One possible explanation is that asymmetric lens positioning and nonuniform tear forces may modify the treatment zone boundary along the direction of lens displacement. When an orthokeratology lens undergoes sustained directional translation during sleep, non coaxial hydrodynamic forces exert intense asymmetric shear stress on the corneal epithelium. This localized mechanical compression forcefully truncates the treatment zone boundary along the exact vector of lens displacement, physically shortening the geometric diameter in that specific meridian. Second, preexisting baseline corneal anatomical asymmetry induces an asymmetric distribution of hydrodynamic stress right from the initiation of lens wear. This uneven mechanical environment generates a lateral vector force, thereby guiding the lens to slide along the path of least resistance. However, the precise hydrodynamic and cellular level mechanisms remain hypothetical and warrant further experimental investigation.

Our results revealed significant differences in the TZA among the four groups. Further subgroup analysis revealed no significant differences in the TZA between the CRT-S and CRT-L groups, the CRT-S and VST-S groups, or the CRT-L and VST-S groups (adjusted $P > 0.05$). Although we observed that the overall TZA for the VST designs was greater than that for the CRT designs, the VST-S group had a BC zone of 5.5 mm, whereas the CRT-S group had a BC zone of 5.0 mm. This suggests that the differences in the TZA between different lens designs with small BC zones require further verification. However, for the VST-L and CRT-L groups, both with 6.0 mm BC zones, the TZA difference was significant (10.52 ± 2.31 vs. 8.16 ± 2.17, $P < 0.001$). This disparity may originate from the fundamental differences in lens geometry, where the VST features multiple curve segments joined together, whereas the CRT utilizes a mathematically continuous sigmoidal curve profile. These distinct geometric architectures may alter the volume of tear pooling within the reverse curve zone. According to Meng's research, CRT lenses exhibit greater fluid dynamic tension within the return zone but exert less mechanical pressure on the central cornea beneath the base curve.[27] Consequently, the post wear epithelial thickness within the mid periphery in the CRT group is identical to or greater than that in the VST group. Rather than expanding the treatment area, this highly concentrated fluid force and robust peripheral epithelial remodeling under the CRT design may act as a strict hydraulic barrier, effectively confining the treatment zone boundary and preventing outward expansion.[27–29] This finding further suggests that, beyond the core design parameters of lens type and BC zone diameter, TZA formation and regulation were influenced by multiple interacting factors.

Previous studies on the factors influencing the TZA have often focused on static corneal morphological data. They largely assumed that preoperative corneal shape was the key predetermined factor for the TZA: Sun et al. reported that the TZA was significantly correlated with baseline SE and axial length;[30] Li et al. reported that preoperative SE and flat keratometry were significantly correlated with the TZA;[31] Gruhl et al. also reported a correlation between SE and treatment zone size;[32] Ding et al. confirmed that the TZA was only correlated with corneal eccentricity and corneal height differences.[33] Our results revealed that lens design, BC zone diameter, TZD, preoperative p, Δkm, ΔCCT, and Δp were significantly correlated with the TZA. Multiple linear regression analysis further confirmed that Δkm, TZD, Δp, preoperative p, and BC zone diameter were independent factors influencing the TZA. This model explained 73.0% of the variance in TZA size ($R^2 = 0.730$). However, because axial elongation and refractive progression were not modeled as outcomes, this R^2 value should not be interpreted as evidence of predictive performance for myopia control efficacy. Notably, Δkm had the most substantial effect on TZA (Standardized Coefficients = 0.963, $P < 0.001$). These findings confirm that, in addition to lens parameters and preoperative corneal morphology, the TZD and dynamic postoperative corneal remodeling process are highly correlated with TZA formation. Regarding the underlying mechanisms, we propose that Δkm represents the primary longitudinal expansion force, wherein a larger required myopia correction drives a greater volume of central epithelial cells to displace outwards, thereby expanding the treatment zone. However, the spatial redistribution profile of this displaced tissue is actively moderated by both preoperative p and Δp. Specifically, preoperative p serves as an anatomical predetermining factor, where a higher baseline value leads to a larger TZA. Crucially, when holding Δkm constant within the multiple regression framework, Δp emerges as a significant negative predictor of TZA size. We speculate that a larger Δp reflects a more abrupt, high density epithelial accumulation localized tightly within the paracentral return zone, which functions to confine the reshaping profile and thereby constricts the extent of the treatment zone.[19,34]

This finding reminds clinicians that for patients with a high preoperative p value, where significant changes in corrective curvature was expected, simply reducing the BC zone size might not achieve the ideal small TZA. Instead, further adjustments to lens fitting parameters, such as lens tightness or sagittal height, may be needed. These changes can alter the lens's corneal remodeling capability, controlling the magnitude of change in km and p, ultimately leading to a stable, smaller TZA. Our study did not find a correlation between the TZA and preoperative SE or km. This might be due to the multifactorial nature of myopia. Patients with the same SE can have different preoperative corneal curvatures and asphericities. Consequently, the reshaping ability of OK lenses also differs.

Simultaneously, the relationship between TZA and TZD should be interpreted within a broader optical and clinical context. In the present multivariable model, greater TZD was independently associated with a larger TZA, indicating a close relationship between treatment zone decentration and treatment zone morphology. Recent evidence suggests that orthokeratology generally shifts peripheral refraction toward

myopic defocus, particularly at approximately 30 degrees of retinal eccentricity, and this optical change is considered one of the principal mechanisms potentially contributing to the inhibition of axial elongation.[35] Previous studies have further shown that treatment zone decentration may alter the spatial distribution of peripheral refraction and higher order aberrations. In particular, temporal decentration may shift portions of the mid peripheral steepened region closer to the pupillary axis, thereby increasing myopic defocus within selected retinal regions.[11,22,26,36] However, allowing unchecked decentration solely for the sake of axial inhibition is clinically unacceptable, as excessive lens displacement escalates the risks of corneal epithelial staining, localized mechanical injury, and degraded visual quality.[37–39] Therefore, treatment zone decentration should be regarded as a potential clinical trade off between peripheral optical effects and the preservation of central visual quality, lens stability, patient comfort, and corneal integrity, rather than as a fitting objective that should be deliberately maximized. Although a certain degree of decentration may be clinically acceptable when satisfactory visual acuity, stable daytime vision, patient comfort, and corneal health are maintained, an optimal and safe range of decentration has not yet been established. Moreover, because peripheral refraction, higher order aberrations, visual quality, axial elongation, and myopia progression were not directly evaluated in the present study, the observed association between TZD and treatment zone morphology should be interpreted as a potential structural correlate of peripheral optical changes rather than direct evidence of improved myopia control efficacy. Future prospective studies integrating peripheral refraction, retinal image quality, corneal health, and axial length outcomes are required to determine whether specific patterns and magnitudes of decentration provide a favorable balance between potential myopia control effects and clinical safety.

Our study has several limitations. First, this was a retrospective study with a relatively limited sample size. Second, our investigation of epithelial remodeling was not based on direct epithelial measurements. This finding was inferred from changes in total corneal thickness. Third, we analyzed data from only the one-year follow-up. This cannot reflect the long-term dynamic changes in the TZA. Fourth, owing to clinical sample limitations, we did not include patients whose VST lenses had a 5.0 mm BC zone. Thus, we could not clarify TZA differences between lens designs at this specific BC diameter. The existing research findings on such differences were inconsistent.[31,40] Finally, a notable limitation inherent in our retrospective design is that the allocation between VST and CRT lens designs was not randomly assigned. In routine clinical practice, practitioners typically select a specific lens design based on the baseline corneal characteristics of the patient. However, it is worth noting that all critical baseline demographic characteristics and ocular parameters were well balanced among the four groups with no statistically significant differences (Table 2). Furthermore, lens design was also excluded from the multivariate linear regression model. Future research should employ large sample, prospective cohort studies. The incorporation of technologies such as anterior segment OCT and ultrasound pachymetry for multiple time point measurements will help further explore the correlations between these parameters and the TZA.

Conclusion

This study confirms that R can be used to measure OK lens treatment zone parameters effectively, and the results were consistent with those of MATLAB. Treatment zone decentration tended to align with the semi-minor axis of the fitted treatment zone ellipse, and greater ellipse eccentricity was associated with greater TZD. When the BC zone is 6.0 mm, VST-designed OK lenses produce a larger TZA than CRT-designed lenses do. Δkm, TZD, Δp, preoperative p, and BC zone diameter were independent factors influencing the TZA, and Δkm had the most substantial effect. Clinicians should carefully consider these factors during OK lens fitting. These findings improve the characterization of treatment zone morphology and may help clinicians anticipate morphological outcomes during individualized orthokeratology lens fitting

Author contributions

XL, YX, ZZ and LZ: design the study, data acquisition and analysis, manuscript writing; JZ: data acquisition and analysis; LZ: final approval of the manuscript.

Ethics approval and consent to participate

This study was conducted in strict adherence to the ethical principles outlined in the World Medical Association Declaration of Helsinki (https://www.wma.net/policies-post/wma-declaration-of-helsinki/). Given the retrospective nature of the study, the Institutional Review Board (IRB) of The Third People's Hospital of Dalian University of Technology waived the requirement for written informed consent from participants, in compliance with the relevant national ethical regulations for retrospective medical research in China. All procedures involving human participants were performed in a manner that protected their privacy, confidentiality, and rights.

Funding

This study was supported by National Natural Science Foundation of China (82171032); Science and Technology Innovation Fund Project of Dalian (2023JJ12SN034); Major Dalian Peak Project (2022ky-01, 2022ky-02); Liaoning Province Science and Technology Plan Joint Program (2024JH2/102600030); the Fundamental Research Funds for the Central Universities, China (DUT25YG270).

Consent for publication

Not Applicable. This study does not contain any identifying images, personal information, or clinical details that could compromise the anonymity of participants.

Data availability

The data that support the findings of this study are available from the authors but restrictions apply to the availability of these data. Given that the data involve personal clinical information and medical records of research participants, they are subject to privacy protection regulations and ethical review requirements approved by the research ethics committee. Thus, the data are not publicly available. Data are available from the first author (Xinda Li) upon reasonable request and with permission from the Ethics Committee of The Third People's Hospital of Dalian University of Technology.

Declaration of competing interest statement

The authors declare that there are no conflicts of interest regarding the publication of this paper.

References

1. Gao J, et al. Analysis of refractive development characteristics in school-age children based on biometric measurements: a cross-sectional study involving 12,025 primary school students from Xingtai City. *Front Public Health*. 2025;13:1660018.
2. Holden BA, et al. Global prevalence of myopia and high myopia and temporal trends from 2000 through 2050. *Ophthalmology*. 2016;123(5):1036–1042.
3. Pärssinen O. Factors associated with the high prevalence of myopia and its decrease-a historical review. *Acta Ophthalmol*. 2025;103(8):879–890.
4. Ikuno Y. Overview of the complications of high myopia. *Retina*. 2017;37(12):2347–2351.

5. Li X, et al. Update on orthokeratology in managing progressive myopia in children: efficacy, mechanisms, and concerns. *J Pediatr Ophthalmol Strabismus*. 2017;54(3):142–148.
6. Lipson MJ, Boland B, McAlinden C. Vision-related quality of life with myopia management: a review. *Cont Lens Anterior Eye*. 2022;45(3):101538.
7. Sarkar S, Khuu S, Kang P. A systematic review and meta-analysis of the efficacy of different optical interventions on the control of myopia in children. *Acta Ophthalmol*. 2024;102(3):e229–e244.
8. Tabernero J, et al. Functional optical zone of the cornea. *Invest Ophthalmol Vis Sci*. 2007;48(3):1053–1060.
9. Pauné J, et al. The role of back optic zone diameter in myopia control with orthokeratology lenses. *J Clin Med*. 2021;10(2).
10. Guo B, et al. One-year results of the variation of orthokeratology lens treatment zone (VOLTZ) study: a prospective randomised clinical trial. *Ophthalmic Physiol Opt*. 2021;41(4):702–714.
11. Yu J, Zhou Y. Effect of lens deviation on peripheral defocus and optic quality in adolescents with moderate and severe myopia. *Eye Contact Lens*. 2024;50(9):375–383.
12. Li X, et al. Efficacy of small back optic zone design on myopia control for corneal refractive therapy (CRT): a one-year prospective cohort study. *Eye Vis (Lond)*. 2023;10(1):47.
13. Masuadi E, et al. Trends in the usage of statistical software and their associated study designs in health sciences research: a bibliometric analysis. *Cureus*. 2021;13(1):e12639.
14. Choueiry G. Statistical software popularity in 40,582 research papers [Internet]. *Quantifying Health*. 2021. [cited 2026 Jul 18]. Available from: https://quantifyinghealth.com/statistical-software-popularity-in-research/.
15. Choo J, Caroline P, Harlin D. How does the cornea change under corneal reshaping contact lenses? *Eye Contact Lens*. 2004;30(4):211–213. discussion 218.
16. Choo JD, et al. Morphologic changes in cat epithelium following continuous wear of orthokeratology lenses: a pilot study. *Cont Lens Anterior Eye*. 2008;31(1):29–37.
17. Reinstein DZ, et al. Epithelial, stromal, and corneal pachymetry changes during orthokeratology. *Optom Vis Sci*. 2009;86(8):E1006–14.
18. Weng T, et al. Changes in corneal epithelial thickness and higher-order aberrations treated with a newly designed orthokeratology lens. *Eye Contact Lens*. 2025;51(9):423–429.
19. Zhou J, et al. Thickness profiles of the corneal epithelium along the steep and flat meridians of astigmatic corneas after orthokeratology. *BMC Ophthalmol*. 2020;20(1):240.
20. Wan K, et al. Corneal thickness changes in myopic children during and after short-term orthokeratology lens wear. *Ophthalmic Physiol Opt*. 2021;41(4):757–767.
21. Chu M, et al. Is orthokeratology treatment zone decentration effective and safe in controlling myopic progression? *Eye Contact Lens*. 2023;49(4):147–151.
22. Chen R, et al. The effect of treatment zone decentration on myopic progression during Or-thokeratology. *Curr Eye Res*. 2020;45(5):645–651.
23. Vincent SJ, et al. CLEAR - orthokeratology. *Cont Lens Anterior Eye*. 2021;44(2):240–269.
24. Chen M, et al. Analysis of anterior corneal surface shape after replacing orthokeratology lenses carrying a small base curve diameter. *Front Neurosci*. 2024;18:1424394.
25. Li Z, et al. Predictive role of paracentral corneal toricity using elevation data for treatment zone decentration during orthokeratology. *Curr Eye Res*. 2018;43(9):1083–1089.
26. Ding W, et al. Effects of orthokeratology lens decentration induced by paracentral corneal asymmetry on axial length elongation. *Eye Contact Lens*. 2023;49(5):181–187.
27. Meng Z, et al. Short-term changes in epithelial and optical redistribution induced by different orthokeratology designs. *Eye Contact Lens*. 2023;49(12):528–534.
28. Swarbrick HA. Orthokeratology review and update. *Clin Exp Optom*. 2006;89(3):124–143.
29. Tahhan N, et al. Comparison of reverse-geometry lens designs for overnight orthokeratology. *Optom Vis Sci*. 2003;80(12):796–804.
30. Sun L, et al. Biometric factors and orthokeratology lens parameters can influence the treatment zone diameter on corneal topography in corneal refractive therapy lens wearers. *Cont Lens Anterior Eye*. 2023;46(1):101700.
31. Li J, et al. Long-term variations and influential factors of the treatment zone of wearing orthokeratology lenses. *Cont Lens Anterior Eye*. 2023;46(4):101867.
32. Gruhl J, et al. Factors influencing treatment zone size in orthokeratology. *Cont Lens Anterior Eye*. 2023;46(4):101848.
33. Ding W, et al. The effect of the back optic zone diameter on the treatment zone area and axial elongation in orthokeratology. *Cont Lens Anterior Eye*. 2024;47(2):102131.
34. Swarbrick HA, Wong G, O'Leary DJ. Corneal response to orthokeratology. *Optom Vis Sci*. 1998;75(11):791–799.
35. Queirós A, Pinheiro I, Fernandes P. Peripheral defocus in orthokeratology myopia correction: systematic review and meta-analysis. *J Clin Med*. 2025;14(3):662.
36. Zhang S, et al. Effect of treatment zone decentration on axial length growth after orthokeratology. *Front Neurosci*. 2022;16:986364.
37. Xue M, et al. Two-dimensional peripheral refraction and higher-order wavefront aberrations induced by orthokeratology lenses decentration. *Transl Vis Sci Technol*. 2023;12(10):8.
38. Li J, et al. Predictive role of corneal Q-value differences between nasal-temporal and superior-inferior quadrants in orthokeratology lens decentration. *Medicine (Baltimore)*. 2017;96(2):e5837.
39. Guo B, Cho P, Efron N. Microcystic corneal oedema associated with over-wear of decentred orthokeratology lenses during COVID-19 lockdown. *Clin Exp Optom*. 2021;104(6):736–740.
40. Jing S, Yan H, Wan Y. Comparison of two designs of orthokeratology lenses with smaller back optic zone diameters in myopia control. *Ophthalmic Physiol Opt*. 2025;45(6):1525–1533.